



# Elevated circulating pregnane X receptor as a novel diagnostic biomarker in hepatocellular carcinoma

Balasubramaniyan Vairappan<sup>1\*</sup> , Tanya Mishra<sup>1</sup> , Biju Pottakkat<sup>2</sup> 

<sup>1</sup>Department of Biochemistry, Jawaharlal Institute of Postgraduate Medical Education and Research, Puducherry 605006, India

<sup>2</sup>Department of Surgical Gastroenterology, Jawaharlal Institute of Postgraduate Medical Education and Research, Puducherry 605006, India

**\*Correspondence:** Balasubramaniyan Vairappan, Department of Biochemistry, Jawaharlal Institute of Postgraduate Medical Education and Research, Dhanvantari Nagar, Puducherry 605006, India. [balasubramaniyan.v@jipmer.edu.in](mailto:balasubramaniyan.v@jipmer.edu.in)

**Academic Editor:** Jian-Guo Chen, Qidong Liver Cancer Institute, China

**Received:** April 29, 2025 **Accepted:** September 1, 2025 **Published:** September 25, 2025

**Cite this article:** Vairappan B, Mishra T, Pottakkat B. Elevated circulating pregnane X receptor as a novel diagnostic biomarker in hepatocellular carcinoma. *Explor Dig Dis.* 2025;4:100594. <https://doi.org/10.37349/edd.2025.100594>

## Abstract

**Aim:** Hepatocellular carcinoma (HCC) poses a significant global health threat. The pregnane X receptor (PXR) is a central regulator of xenobiotic metabolism and plays a key role in mediating cellular resistance to anti-tumor drugs in HCC. Indeed, the precise role of PXR in HCC pathogenesis remains unclear. This study aimed to investigate blood and hepatic PXR levels and their association with inflammation in HCC patients. Additionally, we assessed the diagnostic potential of PXR in HCC patients compared to control subjects.

**Methods:** Following approval by the Institute Ethical Committee, 40 HCC patients and 40 healthy volunteers were enrolled in this study. Baseline patient characteristics, serum alpha-fetoprotein (AFP), and biochemical parameters were analyzed. Serum levels of PXR, tumor necrosis factor alpha (TNF- $\alpha$ ), and interleukin (IL)-1 $\beta$  were measured using ELISA. The hepatic expression of phosphorylated nuclear factor kappa B (NF $\kappa$ B) and PXR proteins was analyzed by western blotting.

**Results:** When compared to control subjects, serum PXR levels were increased in HCC cases ( $1.34 \pm 0.16$  vs.  $4.09 \pm 0.33$ ;  $P < 0.0001$ ). Similarly, hepatic PXR expression was increased in HCC tissues. Moreover, HCC patients exhibited elevated inflammatory cytokines and a deranged hepatobiliary profile compared to controls.

**Conclusions:** Elevated serum PXR levels in HCC patients were positively correlated with inflammation. Notably, serum PXR demonstrated greater sensitivity and specificity in diagnosing HCC. These findings suggest that PXR may serve as a plausible biomarker in the diagnosis of HCC.

## Keywords

inflammation, liver cancer, pregnane X receptor, serum biomarker



## Introduction

Liver cancer remains a major contributor to the global cancer burden and ranks third in estimated cancer-related deaths, driven by the rising prevalence of metabolic disorders, increasing alcohol consumption, and the shifting epidemiology resulting from advances in hepatitis B virus (HBV) vaccination and effective antiviral therapies for hepatitis C virus (HCV) [1]. Hepatocellular carcinoma (HCC), which accounts for approximately 75% of primary liver cancer cases and deaths worldwide [2], has a complex pathogenesis involving various genetic and epigenetic alterations. HCC incidence varies geographically worldwide, with approximately 900,000 new cases reported, with around 760,000 deaths attributed to the disease. Notably, the expected incidence of HCC is projected to increase by 55% from 2020 to 2040 [3]. The etiology of HCC is primarily linked to chronic inflammation caused by hepatitis B and C viral infections, as well as cirrhosis [4]. Although several candidate drugs have failed in clinical trials as frontline treatments for HCC, a number of kinase inhibitors and immunotherapeutics have been approved by the U.S. Food and Drug Administration (FDA). The first systemic drug approved as a standard frontline therapy for HCC was sorafenib, a kinase inhibitor targeting multiple signaling pathways [5]. However, Feng et al. [6] demonstrated that while sorafenib is initially effective in some HCC patients, the majority eventually develop resistance. This resistance is partly attributed to sorafenib's activation of the pregnane X receptor (PXR), a nuclear hormone receptor [6]. PXR functions as a cellular xenobiotic sensor, playing a protective role by promoting the clearance of potentially harmful foreign substances. Notably, its expression is predominantly observed in hepatic and intestinal tissues [7, 8].

Beyond its well-established role in chemoresistance, the PXR has emerged as a key regulator of various metabolic pathways [7]. In addition, PXR influences several cancer-related processes, including cell cycle arrest, inflammation, and angiogenesis, which are hallmarks of carcinogenesis [7, 9]. Interestingly, PXR expression varies significantly across different cancer types [10]. Overexpression of PXR in breast, esophageal, and bone cancers has been linked to the upregulation of multidrug resistance (MDR) genes, which can facilitate cancer progression [11]. Conversely, in colon, prostate, and cervical cancers, PXR expression is markedly reduced. Restoration of its activity in these contexts has been shown to suppress cell proliferation, suggesting a tumor-suppressive function [10]. However, the role of PXR in HCC remains poorly defined. In HuH7 cells, PXR activation has been reported to suppress cell proliferation and migration [12]. In contrast, studies in HepG2 cells have shown that PXR activation promotes changes in cell morphology and enhances migration via activation of the p38 MAPK signaling pathway [13]. Additionally, the inflammatory microenvironment associated with HCC leads to the activation of Kupffer cells, which release proinflammatory cytokines such as tumor necrosis factor alpha (TNF- $\alpha$ ) and interleukin (IL)-1 $\beta$  via the nuclear factor kappa B (NF $\kappa$ B) pathway. In this study, we aimed to assess the PXR levels in both systemic circulation and liver tissue, examine their relationship with key inflammatory markers in HCC, and evaluate their potential as a diagnostic biomarker by comparing HCC patients with apparently healthy individuals.

## Materials and methods

### Human HCC

This case-control study was conducted from September 2018 to February 2020 in the Department of Biochemistry, in collaboration with the Department of Surgical Gastroenterology at the Jawaharlal Institute of Postgraduate Medical Education and Research (JIPMER), Puducherry, India. Ethical approval was obtained from the Institute Ethics Committee (JIP/IEC/2018/0282), and the study adhered to the Indian Council of Medical Research (ICMR) biomedical guidelines and the Declaration of Helsinki. Written informed consent was obtained from all participants prior to enrollment.

### Study participants

Consecutive patients were recruited. Both male and female participants aged 20–60 years were enrolled and divided into two groups: healthy controls ( $n = 40$ ) and HCC patients ( $n = 40$ ). Controls were selected

based on normal liver function tests and the absence of any recent infections or tumors. HCC patients meeting the inclusion criteria in line with the European Association for the Study of the Liver (EASL) criteria. Moreover, critically ill patients and those with rare variants like fibrolamellar carcinoma were excluded, as this subtype can complicate HCC diagnosis. Non-invasive imaging techniques were used to distinguish fibrolamellar carcinoma from classical HCC. HCC diagnosis was based on ultrasonography and confirmed through CT or MRI, supported by elevated alpha-fetoprotein (AFP) levels or histopathological analysis. Tumor characteristics, including lesion count, vascular invasion, and metastasis, were assessed via CT or MRI and reviewed by an independent radiologist at JIPMER. Confirmation of HCC was done by biopsy or ultrasound-guided fine needle aspiration cytology (FNAC), interpreted by a blinded pathologist. Disease severity was evaluated using the Child-Pugh score, and staging was conducted according to the Barcelona Clinic Liver Cancer (BCLC) system.

### **Sampling procedure**

All patients' demographic and clinical data were collected at admission. Furthermore, approximately 5 mL of blood was collected from both control subjects and HCC patients into clot activator tubes (BD Vacutainer, REF 369032) and allowed to stand for one hour. The samples were then centrifuged at  $1,000 \times g$  for 10 min at 4°C to separate the serum. Routine biochemical analyses were performed immediately using the fresh serum, while the remaining samples were aliquoted and cryopreserved at -80°C for further analysis.

Liver tumor tissues and adjacent non-tumorous tissues (histologically confirmed as controls) were obtained from HCC patients undergoing hepatectomy as part of their treatment protocol. Each resected tissue sample was divided: one portion was fixed in 10% neutral buffered formalin (NBF) for histological examination, and the other was snap-frozen in liquid nitrogen and stored at -80°C for molecular studies.

### **Analysis of biochemical parameters**

Liver function markers, including bilirubin, total protein, albumin, alanine aminotransferase (ALT), aspartate aminotransferase (AST), alkaline phosphatase (ALP), and gamma-glutamyltransferase ( $\gamma$ GT), were measured using commercially available kits (Beckman Coulter Ireland, Inc.) on a Beckman Coulter AU5800 autoanalyzer (USA), following the manufacturer's instructions. Prothrombin time (PT) and international normalized ratio (INR) were assessed using a chemiluminescence immunoassay system (Siemens ADVIA Centaur CP). Serum AFP levels were quantified by chemiluminescence using the UniCel Dxl 600 Access Immunoassay System (Beckman Coulter, USA; 33210).

### **Assessment of PXR and proinflammatory cytokines**

Serum PXR and IL-1 $\beta$  concentrations were estimated using sandwich ELISA kits from FineTest, Wuhan Fine Biotech Co., Ltd, Wuhan, China (PXR: Cat. No. EH1200; IL-1 $\beta$ : Cat. No. EH0185), and serum TNF- $\alpha$  was assessed using the human TNF- $\alpha$  ELISA kit (Cat. No. KB1145; Krishgen Biosystems, USA) as per the manufacturer's instructions. Briefly, standards and serum samples were added to microplate wells pre-coated with target-specific antibodies. After incubation and washing to remove unbound substances, a biotinylated detection antibody and streptavidin-HRP conjugate were added sequentially. The resulting colorimetric reaction, following substrate addition, was measured at the appropriate wavelength using a microplate reader (Spectra max Plus 384; Serial No: AMNR06890; Thermo Fisher Scientific Inc.). Concentrations of PXR, TNF- $\alpha$ , and IL-1 $\beta$  were calculated by comparing absorbance values to a standard curve generated for each target analyte.

### **Receiver operating characteristic (ROC) curve analysis**

ROC curve analysis was conducted using GraphPad Prism version 10 (San Diego, CA, USA) and MedCalc (version 23.3.7; MedCalc Software Ltd) to evaluate the diagnostic performance of AFP and PXR in HCC patients. The cut-offs for PXR, AFP were chosen based on ROC analysis and Youden's index, providing strong sensitivity and specificity for distinguishing HCC from non-HCC individuals.

## Western blotting

Total protein was extracted from tumorous and non-tumorous liver tissues of HCC patients using ice-cold RIPA buffer (Cat. # 786-489; G-Biosciences, USA) containing a protease inhibitor cocktail and PMSF (Cat. # P8340 and 11359061001, respectively; Sigma-Aldrich, USA). Protein concentrations were determined using the Pierce Coomassie Plus (Bradford) protein assay kit (Cat. # 23236; Thermo Fisher Scientific, USA). Protein samples (~30 µg) were separated by SDS-PAGE on 7.5% and 10% polyacrylamide gels and transferred to nitrocellulose membranes (S045A330R; Advantec, Japan). Membranes were blocked and incubated with rabbit polyclonal anti-PXR (Cat. # A1583; ABclonal, USA) and rabbit monoclonal phosphorylated anti-NFκB-p65 (Cat. # 3033 1:1,000; Cell Signaling, UK), and mouse monoclonal anti-β-actin (Cat. # AC004; ABclonal, USA) antibodies at recommended dilutions. After overnight incubation, membranes were probed with HRP-conjugated goat anti-rabbit or goat anti-mouse secondary antibodies (Cat. # 405306; BioLegend, USA). Protein bands were visualized using an enhanced chemiluminescent substrate (Cat. # 32209; Thermo Fisher Scientific, USA) and imaged on a ChemiDoc XRS+ system (Cat. # 1708265; Bio-Rad, USA). Densitometry analysis was performed using Image Lab software (V 6.1.0; Bio-Rad, USA), and target bands were normalized to β-actin.

## Histopathology and immunohistochemistry

Paraffin blocks of 10% NBF-fixed tumorous and non-tumorous liver tissues were prepared. Serial 5 µm sections were obtained using an automated microtome (Cat. # 149AUTO000C1; Leica Biosystems) and stained with hematoxylin and eosin (H&E). Histological characteristics of the HCC tumor and non-tumorous tissues (control liver) were assessed by an independent, blinded pathologist from the Department of Pathology, JIPMER. For immunohistochemistry (IHC), tissue sections were placed on silane-coated slides, deparaffinized in xylene, and rehydrated. Endogenous peroxidase activity was blocked with 3% H<sub>2</sub>O<sub>2</sub> (Cat. # 88597; Sigma-Aldrich, USA) and rinsed with phosphate-buffered saline (PBS). Antigen retrieval was performed by incubating sections in citrate buffer (pH 6.0) (Cat. # ALF-J63950-AP; Thermo Fisher Scientific, USA) at 110°C for 10 min. The sections were then blocked with 2.5% normal horse serum for 20 min and incubated overnight with rabbit polyclonal anti-PXR (1:100, Cat. # A1583; ABclonal, USA) at 4°C. After washing with PBS, sections were incubated with ImmPRESS Universal Polymer Reagent (MP-7500; Vector Labs, USA) for 30 min at room temperature. PXR localization was detected using the ImmPACT DAB kit (SK4105; Vector Labs, USA), and sections were counterstained with hematoxylin. Negative controls were included using a no-primary antibody condition. Finally, sections were dehydrated, mounted with Histomount (Cat. # 008030; Thermo Fisher Scientific, USA), and photographed using an EVOS FLc imaging system (Cat. # AME3300; Life Technologies, USA).

## Statistical analysis

Data were analyzed using GraphPad Prism version 10 (San Diego, CA, USA) and MedCalc (version 23.3.7; MedCalc Software Ltd). Qualitative data are presented as counts and percentages, while quantitative data are expressed as mean ± standard error (SE). A two-tailed unpaired *t*-test or Mann-Whitney *U* test was used to compare cases and controls. Spearman's correlation analysis assessed associations between parameters. ROC curve analysis for AFP and PXR was performed to evaluate diagnostic accuracy in HCC participants. *P* values < 0.05 were considered statistically significant.

## Results

### Clinical and tumor radiological characteristics of HCC cases

**Table 1** shows the clinical and tumor radiological characteristics of HCC patients. The Child-Pugh score was used to assess the disease severity and was distributed as Child class A (60%), Child class B (32.5%), and Child class C (7.5%). BCLC staging was also done for HCC participants and accordingly found to be in stages A (12.5%), B (27.5%), C (55%), and D (5%). Among the HCC participants, 65% had one lesion, 20% had two lesions, 7.5% had three, and 7.5% had multifocal lesions. Hepatic and portal vein invasions were observed in 27.5% and 37.5% of HCC participants, respectively. 22.5% were hepatitis B surface antigen (HBsAg) positive and 17.5% were HCV positive. Cirrhosis was present in 62.5% of HCC participants.

**Table 1. Clinical and tumor radiological characteristics of the study population.**

Characters	N (total 40)	% (total 100)
Child class		
A	24	60.0
B	13	32.5
C	3	7.5
BCLC staging		
Stage A	5	12.5
Stage B	11	27.5
Stage C	22	55.0
Stage D	2	5.0
No. of lesions		
Single lesion	26	65.0
Two lesions	8	20.0
Three lesions	3	7.5
Multifocal lesions	3	7.5
Hepatic vein invasion		
Present	11	27.5
Absent	29	72.5
Metastasis		
Present	2	5.0
Absent	38	95.0
Portal vein invasion		
Present	15	37.5
Absent	25	62.5
Hepatitis infection		
No hepatitis infection	24	60.0
HBsAg positive	9	22.5
HCV positive	7	17.5
Cirrhosis		
Present	25	62.5
Absent	15	37.5

BCLC: Barcelona Clinic Liver Cancer; HBsAg: hepatitis B surface antigen; HCV: hepatitis C virus.

### Liver function parameters in controls and cases

Serum levels of liver function parameters are given in Table 2. Levels of total and direct bilirubin, AST, ALT,  $\gamma$ GT, ALP, PT, and INR increased significantly, while serum albumin level was decreased in HCC cases compared to controls. Furthermore, higher AFP levels ( $P < 0.0001$ ) were observed in HCC cases compared to healthy controls.

**Table 2. Comparison of biochemical parameters in healthy controls and HCC participants.**

Parameters	Healthy controls (n = 40) mean $\pm$ SE	HCC cases (n = 40) mean $\pm$ SE	P-value
Gender (M/F)	29/11	32/8	-
Age (years)	48.9 $\pm$ 8.52	53.8 $\pm$ 6.34	-
BMI (kg/m <sup>2</sup> )	23.46 $\pm$ 4.22	27.62 $\pm$ 5.68	$P < 0.001$
Total bilirubin (mg/dL)	0.47 $\pm$ 0.048	5.57 $\pm$ 1.11	$P < 0.001$
Direct bilirubin (mg/dL)	0.18 $\pm$ 0.015	2.69 $\pm$ 0.57	$P < 0.001$
Total protein (g/dL)	6.638 $\pm$ 0.156	6.81 $\pm$ 0.16	NS
Albumin (g/dL)	3.625 $\pm$ 0.113	3.048 $\pm$ 0.11	$P < 0.001$
AST (IU/L)	27.05 $\pm$ 1.639	188.6 $\pm$ 26.67	$P < 0.001$
ALT (IU/L)	31.03 $\pm$ 3.414	85.66 $\pm$ 18.87	$P < 0.0001$



**Table 2. Comparison of biochemical parameters in healthy controls and HCC participants. (continued)**

Parameters	Healthy controls (n = 40) mean ± SE	HCC cases (n = 40) mean ± SE	P-value
ALP (IU/L)	80.95 ± 6.636	525.2 ± 134.4	<i>P</i> < 0.001
γGT (IU/L)	36.63 ± 5.774	409.2 ± 114.7	<i>P</i> < 0.001
PT (s)	11.69 ± 0.81	15.87 ± 1.05	<i>P</i> < 0.001
INR	1.02 ± 0.024	1.305 ± 0.09	<i>P</i> < 0.001
AFP (ng/mL)	12.60 ± 0.839	508.6 ± 117.2	<i>P</i> < 0.0001

–: No statistical comparison was performed between groups. HCC: hepatocellular carcinoma; SE: standard error; BMI: body mass index; NS: non-significant; AST: aspartate aminotransferase; ALT: alanine aminotransferase; ALP: alkaline phosphatase; γGT: gamma-glutamyltransferase; PT: prothrombin time; INR: international normalized ratio; AFP: alpha-fetoprotein.

### Serum PXR and proinflammatory cytokine concentrations in healthy controls and HCC cases

PXR, TNF-α, and IL-1β serum concentrations were increased (*P* < 0.0001) in HCC cases compared to control subjects (Figure 1A–C). Furthermore, serum levels of PXR showed a positive correlation with TNF-α and IL-1β (*r* = 0.456, *P* < 0.001; *r* = 0.476, *P* < 0.0001 respectively; Figure 1D and E). Moreover, a positive correlation was noted between PXR and elevated γGT levels (*r* = 0.490, *P* < 0.0001; Figure 1F and G). Notably, subgroup analysis among HCC cases revealed that PXR concentration was higher (*P* < 0.05) in alcoholic HCC as compared to non-alcohol-related HCC (Figure 1H). We also observed PXR expression according to BCLC staging in HCC patients (Figure 1I). PXR expression was significantly higher in stage B and stage C compared to stage A (*P* = 0.009 and *P* = 0.001, respectively). Although PXR levels were elevated in stage C compared to stage B, this difference was not statistically significant.

### ROC curve analysis of AFP and PXR

Figure 2 illustrates the ROC curve analysis of AFP and PXR for evaluating their diagnostic performance in HCC participants. AFP at a cut-off value > 18.9 ng/mL achieved an AUC of 0.883, with 83% sensitivity and 88% specificity, yielding a positive likelihood ratio (LR<sup>+</sup>) of 6.6 and a negative likelihood ratio (LR<sup>–</sup>) of 0.2 (Figure 2A). PXR at a cut-off value > 2.014 ng/mL demonstrated an AUC of 0.902, with 83% sensitivity and 90% specificity, corresponding to an LR<sup>+</sup> of 8.3 and an LR<sup>–</sup> of 0.19 (Figure 2B). Figure 2C shows a pairwise comparison of ROC curves between PXR and AFP (ng/mL) using DeLong's test [14]. The comparison between PXR and AFP ROC curves shows a small difference in AUCs (0.0191), with a non-significant *P*-value of 0.7616. The 95% confidence interval for the difference includes zero (–0.104 to 0.142), and the *z* statistic is 0.303, indicating no statistically significant difference in diagnostic performance between PXR and AFP.

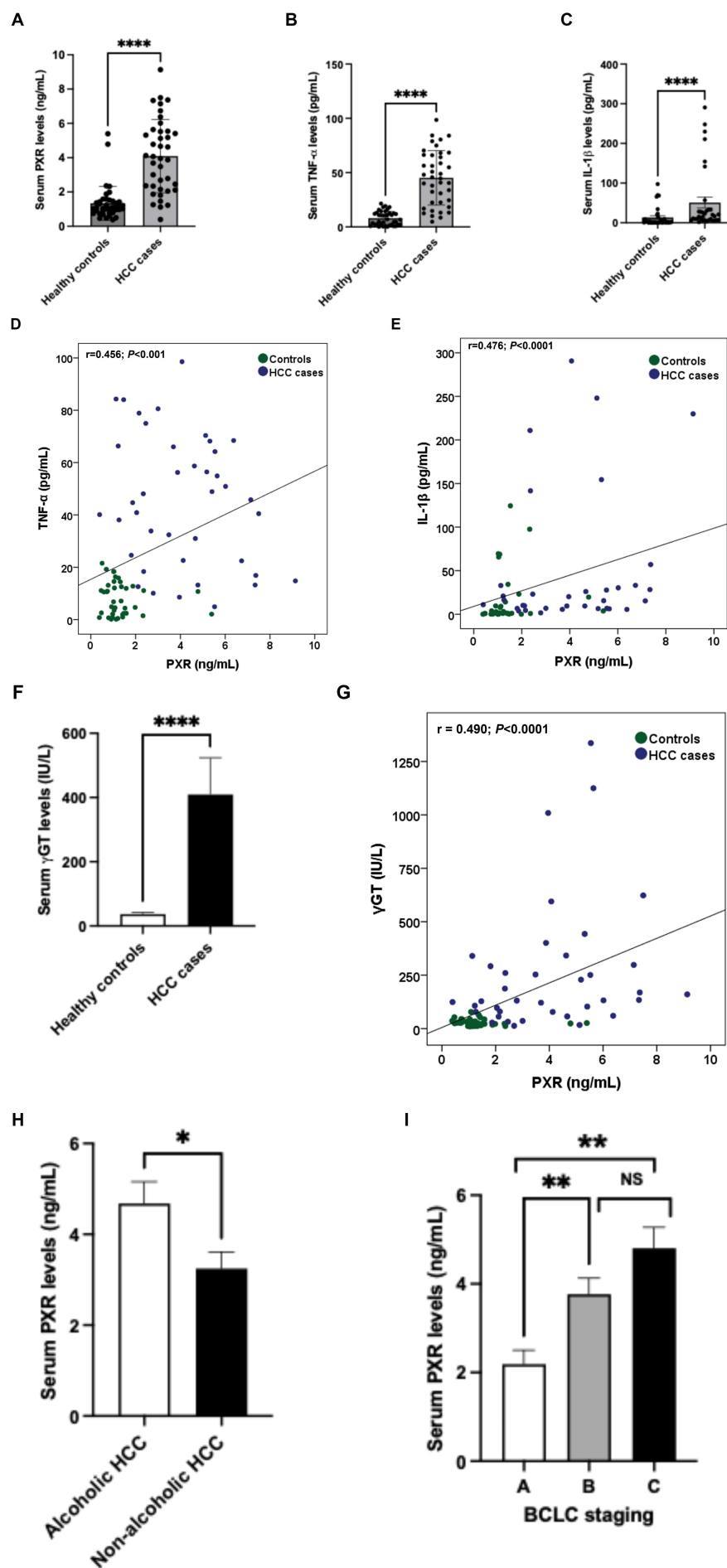
### Expression of PXR in hepatic tumors and non-tumorous tissues

Figure 3A shows the H&E-stained liver section of non-tumorous (control liver) and tumorous tissue obtained from HCC participants. The control liver showed typical hepatic lobular architecture characterized by densely stained hepatocyte cytoplasm with prominent granularity, round nuclei, and nucleoli arranged in regular cords or plates separated by sinusoids. The portal zone included connective tissue, hepatic artery, portal vein, and bile duct. The HCC liver tissue showed classical features of HCC characterized by the presence of malignant cells, thick trabecular cords, well-differentiated and interdigitated with scant basophilic cytoplasm, nuclear overcrowding, and hyperchromatic nuclei.

Figure 3B shows immunostaining of PXR on sections of the control liver and HCC liver. Control liver tissue showed moderate cytoplasmic and focal nuclear PXR positivity, while HCC liver tissue demonstrated strong cytoplasmic and focal nuclear PXR positivity. Figure 3C shows hepatic PXR protein expression by western blot in the control liver and HCC tumor tissues. PXR protein expression was increased (*P* < 0.05) in HCC tumor tissue compared to control liver tissue. Similarly, hepatic phosphorylated NFκB expression was significantly increased in the HCC liver compared to the control liver (Figure 3D).

## Discussion

In this study, systemic PXR concentration was elevated in HCC patients compared to control subjects. We also found increased serum inflammatory cytokines, such as TNF-α and IL-1β levels, in HCC patients



**Figure 1. Serum PXR and proinflammatory cytokine concentrations in control subjects and HCC cases.** Serum PXR (A), TNF- $\alpha$  (B), and IL-1 $\beta$  (C) levels in controls and cases. (D) Correlation between PXR and TNF- $\alpha$  in controls and cases. (E) Correlation between PXR and IL-1 $\beta$  in controls and cases. (F) Serum  $\gamma$ GT levels in controls and cases. (G) Correlation between PXR and  $\gamma$ GT in controls and cases. (H) Serum PXR levels between non-alcohol-related and alcohol-related subgroups of cases. (I) Serum PXR levels in different BCLC staging of HCC patients. All the data are expressed as mean  $\pm$  SE. The comparison between groups was performed using either a two-tailed unpaired *t*-test or the Mann-Whitney *U* test, as appropriate. Spearman's correlation was performed to study the association between PXR with TNF- $\alpha$ , IL-1 $\beta$ , and  $\gamma$ GT levels. \*\*\*\*:  $P < 0.0001$  compared to controls; \*:  $P < 0.05$ ; \*\*:  $P < 0.01$  compared to BCLC stage A; *r*: correlation coefficient. PXR: pregnane X receptor; HCC: hepatocellular carcinoma; TNF- $\alpha$ : tumor necrosis factor alpha; IL: interleukin;  $\gamma$ GT: gamma-glutamyltransferase; BCLC: Barcelona Clinic Liver Cancer; SE: standard error; NS: non-significant.

compared to control subjects. Additionally, elevated PXR observed in HCC patients was positively correlated with elevated proinflammatory cytokines. Interestingly, elevated systemic PXR concentration positively correlated with elevated  $\gamma$ GT, and the levels were higher in alcoholic HCC than in non-alcoholic HCC. In addition, we observed significantly elevated hepatic PXR expression in tumor tissues compared to adjacent non-tumor liver tissue. Similarly, hepatic inflammation was increased in tumor tissues, as indicated by elevated levels of phosphorylated NF $\kappa$ B.

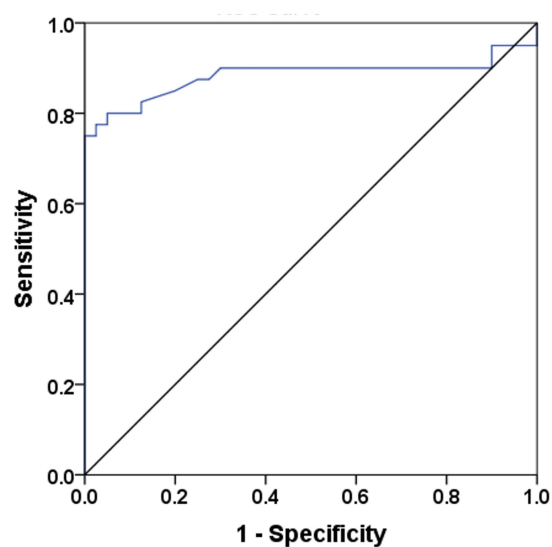
Several studies have implicated PXR in cancer development. In the liver, PXR is expressed not only in hepatocytes but also in Kupffer and hepatic stellate cells [15], with expression levels varying during liver development. In our study, we observed significantly higher hepatic PXR expression in liver tumors compared to non-cancerous tissue. This may reflect differences in PXR activation and hepatocyte proliferation, both of which can promote HCC progression. Although previous *in vivo* and *in vitro* studies reported reduced PXR expression in liver cancer models [9, 11], its pleiotropic roles in HCC remain poorly understood. Notably, Yoshinari [16] demonstrated that the constitutive androstane receptor (CAR), which interacts with PXR, suppresses cell-cycle inhibitor genes, thereby promoting hepatocyte proliferation and HCC progression. Shizu et al. [17] further showed that co-activation of PXR and CAR in mice synergistically induces hepatocyte proliferation and carcinogenesis. PXR overexpression has also been linked to reduced efficacy of anti-cancer drugs such as doxorubicin and sorafenib via TGF- $\beta$ -mediated chemoresistance [18]. In line with this, Feng et al. [6] found that sorafenib treatment activates PXR and its downstream targets (e.g., *CYP3A4* and *MDR1*), promoting drug resistance in HCC patients. Indeed, its potential role in different stages of HCC tumor development needs further investigation. We found significantly increased hepatic PXR expression in HCC cases, consistent with increased distribution of PXR in the cytosol and the nucleus, as evidenced by IHC. Serum PXR levels were also significantly higher compared to healthy controls. Although the sample size for the subgroup analysis was limited, we observed that PXR expression varied with disease stage. Patients in BCLC stages B and C showed significantly higher serum PXR levels compared to those in stage A, suggesting a correlation between PXR expression and disease severity. We speculate that frequent exposure to PXR-activating chemotherapeutics, such as sorafenib and doxorubicin, contributes to this increase. In contrast, diethyl nitrosamine (DEN) or carbon tetrachloride (CCl<sub>4</sub>)-induced mouse models of HCC do not fully capture the complexity of the human tumor microenvironment, treatment history, and disease progression. Thus, the role of PXR in different stages of HCC remains to be fully elucidated and warrants further investigation.

Inflammation plays a key contributory role in the development and progression of HCC, and most incidences of HCC have altered inflammatory marker levels [2]. NF $\kappa$ B is a transcription factor and an important molecule linking chronic inflammation to cancer [19]. Its activity is primarily induced by proinflammatory cytokines such as TNF- $\alpha$  and IL- $\beta$  and bacterial endotoxins. Many clinical studies have shown evidence that NF $\kappa$ B activation occurs in cancer cells and in the tumor microenvironment of HCC [20]. Expression of NF $\kappa$ B within Kupffer cells is fundamental for the development of HCC [21]. Herein, we observed increased hepatic phosphorylated NF $\kappa$ B protein expression in HCC compared to control subjects. We also noted significantly elevated systemic TNF- $\alpha$  and IL- $\beta$  levels in HCC, and these were positively correlated with elevated PXR levels. However, our study differs from previous findings that PXR mitigates inflammation through negative regulation of NF $\kappa$ B [22] and proinflammatory cytokines [11]. Alternatively, IL-1 $\beta$ , IL-6, and TNF- $\alpha$  have been reported to down-regulate PXR expression in mice [23]. Indeed, the role of inflammation in promoting PXR expression in liver cancer needs further investigation.



**A**

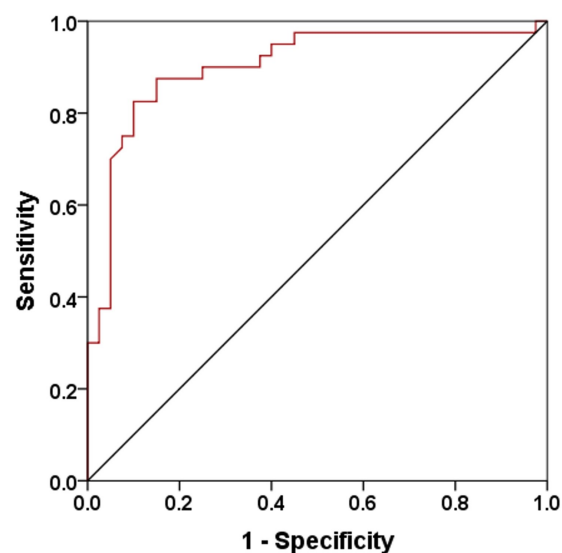
ROC curve of AFP;  $P < 0.0001$



ROC of AFP						
Parameter	Cut-off	AUC	Sensitivity	Specificity	Positive Likelihood Ratio	Negative Likelihood Ratio
AFP	> 18.9 (ng/mL)	0.883	83%	88%	6.6	0.2

**B**

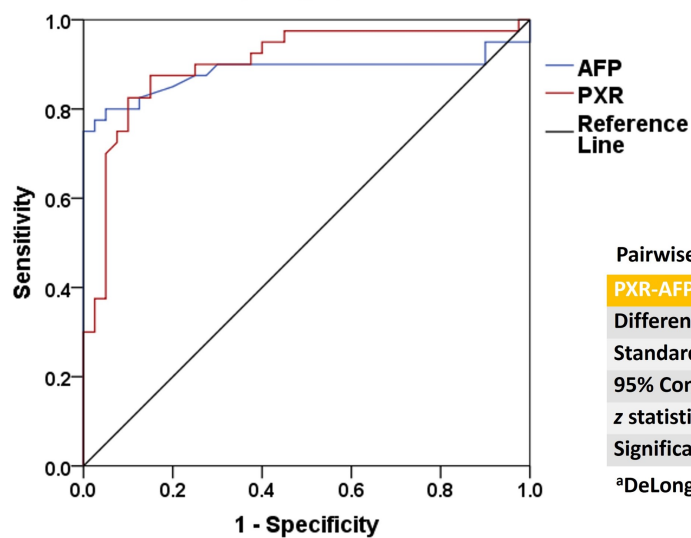
ROC curve of PXR;  $P < 0.0001$



ROC of PXR						
Parameter	Cut-off	AUC	Sensitivity	Specificity	Positive Likelihood Ratio	Negative Likelihood Ratio
PXR	> 2.014 (ng/mL)	0.902	83%	90%	8.3	0.19

**C**

ROC curve



Pairwise comparison of ROC curves

PXR-AFP (ng/mL)

Difference between areas 0.0191

Standard Error <sup>a</sup> 0.0628

95% Confidence Interval - 0.104 to 0.142

z statistic 0.303

Significance level  $P = 0.7616$

<sup>a</sup>DeLong et al., 1988

**Figure 2. The ROC curve analysis of AFP and PXR. (A)** ROC analysis of AFP in the study population. **(B)** ROC analysis of PXR in the study population. **(C)** Pairwise comparison of ROC curves between PXR and AFP (ng/mL) using DeLong's test. All the data are expressed as mean  $\pm$  SE. The comparison between groups was performed using either a two-tailed unpaired *t*-test or the Mann-Whitney *U* test, as appropriate. ROC: receiver operating characteristic; AFP: alpha-fetoprotein; AUC: area under the curve; PXR: pregnane X receptor; SE: standard error.

Our study provides compelling evidence that elevated PXR may serve as a novel diagnostic marker for HCC pathogenesis. Although AFP has been used for this purpose, its limited sensitivity and specificity have restricted its diagnostic effectiveness [24, 25]. In contrast, serum PXR demonstrated higher sensitivity, specificity, and likelihood ratio than AFP in diagnosing HCC. However, the pairwise comparison of ROC curves revealed no statistically significant difference between PXR and AFP in their ability to distinguish HCC from controls. Thus, DeLong's analysis confirms that PXR performs comparably to AFP as a diagnostic marker in this study population. Additionally, elevated serum PXR levels in HCC patients showed a positive correlation with  $\gamma$ GT levels, prompting a subgroup analysis despite the small sample size of alcohol-related HCC cases ( $n = 13$ ). Notably, PXR levels were higher in alcohol-related HCC compared to non-alcohol-related cases. In this context, Choi et al. [26] reported that chronic ethanol exposure significantly upregulated the mRNA levels of PXR, CAR, and the CAR target gene *CYP2B10* in wild-type mice, but not in PXR-null mice. This PXR-dependent response also increased the gene and protein expression of early growth response-1 (EGR-1). EGR-1, in turn, upregulates sterol regulatory element binding protein (*SREBP*)-1c target genes like fatty acid synthase (*FAS*) and *TNF- $\alpha$* , contributing to ethanol-induced steatosis [26]. These findings suggest that PXR signaling plays a key role in alcohol-related liver disease (ALD) and that PXR antagonists may represent a potential therapeutic strategy for ALD. Indeed, increased PXR levels observed in alcohol-induced HCC remain to be investigated. The limitations of the current study are the lack of data on the relationship between PXR and the survival and prognosis of HCC. This study also lacks an external validation cohort, limiting the generalizability of the findings. Moreover, we used a relatively small sample size, which may influence the observed expression levels of PXR, the determined cut-off value for AFP in HCC diagnosis, and the overall diagnostic performance of both biomarkers. PXR levels measured by ELISA may not have been fully accurate; however, in our future studies, we plan to use liquid chromatography-mass spectrometry (LC-MS) for a more precise quantification of PXR in HCC.

In conclusion, to the best of our knowledge, this study is the first to demonstrate that serum PXR levels are significantly elevated in patients with HCC, accompanied by increased hepatic PXR expression. ROC curve analysis further revealed that PXR has strong diagnostic potential, underscoring its promise as a novel biomarker for HCC. Nonetheless, validation through larger, independent cohorts is essential to confirm these findings and establish clinical utility.

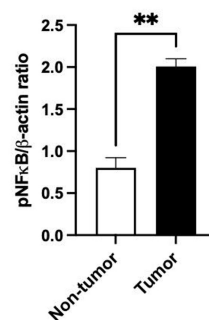
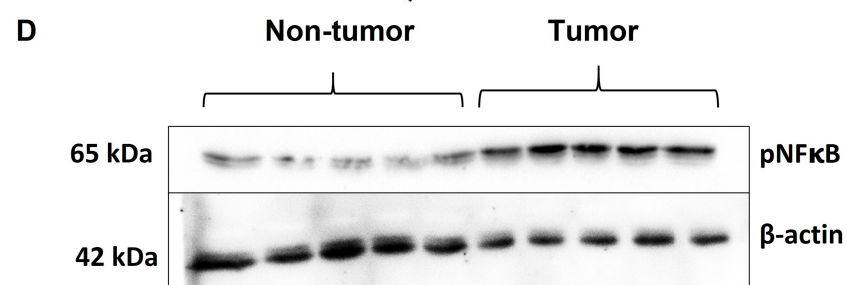
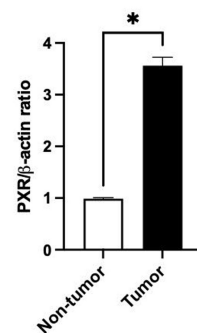
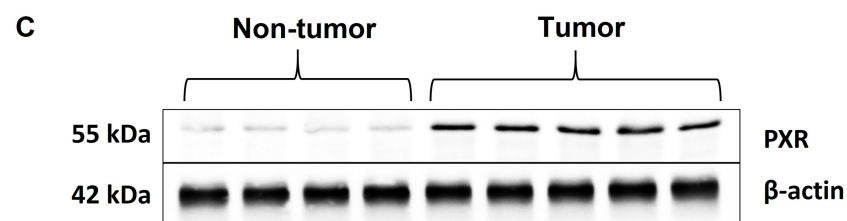
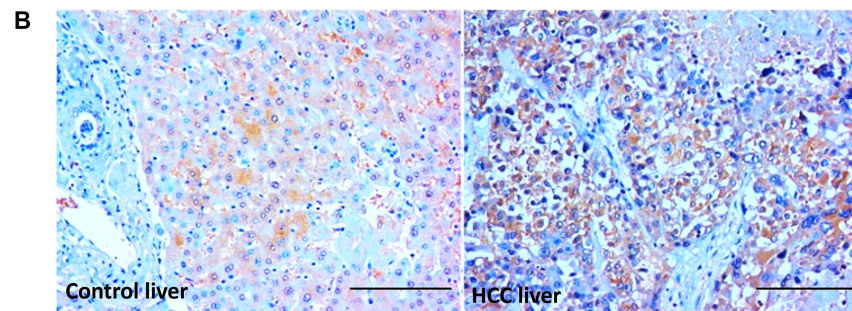
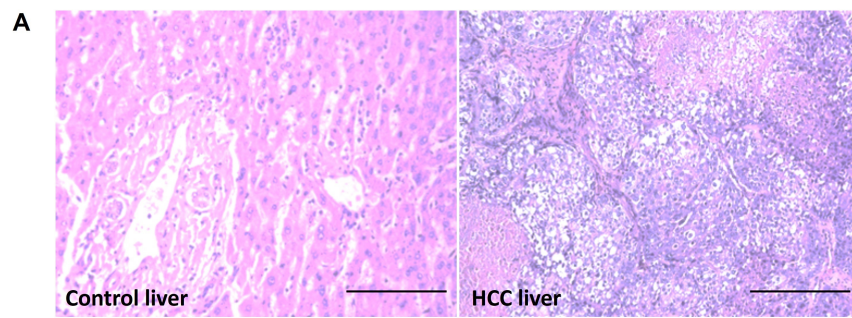


**Figure 3. PXR expression in tumor and non-tumorous liver tissues.** (A) Representative images of H&E-stained liver sections of non-tumorous (control liver) and tumor tissue (HCC liver) from HCC participants (200× magnification; scale bar: 75 μm). (B) Representative images of PXR immunostaining of liver sections of non-tumorous (control liver) and tumor tissue (HCC liver) from HCC participants (200× magnification; scale bar: 75 μm). (C) Hepatic PXR protein expression [non-tumorous tissue (*n* = 4); tumor tissue (*n* = 5)] and (D) hepatic phosphorylated NFκB 65 expression [non-tumorous tissue (*n* = 5); tumor tissue (*n* = 5)] by western blot in non-tumorous and tumor tissue from HCC participants. All the data are expressed as mean ± SE. The comparison between groups was performed using either a two-tailed unpaired *t*-test or the Mann-Whitney *U* test, as appropriate. \*: *P* < 0.05 & \*\*: *P* < 0.01 compared to non-tumor. HCC: hepatocellular carcinoma; PXR: pregnane X receptor; pNFκB: phosphorylated nuclear factor kappa B; H&E: hematoxylin and eosin; SE: standard error.

## Abbreviations

AFP: alpha-fetoprotein

ALD: alcohol-related liver disease

ALP: alkaline phosphatase

ALT: alanine aminotransferase

AST: aspartate aminotransferase

BCLC: Barcelona Clinic Liver Cancer

CAR: constitutive androstane receptor

EGR-1: early growth response-1

H&E: hematoxylin and eosin

HCC: hepatocellular carcinoma

HCV: hepatitis C virus

IHC: immunohistochemistry

IL: interleukin

INR: international normalized ratio

LR<sup>-</sup>: negative likelihood ratio

LR<sup>+</sup>: positive likelihood ratio

MDR: multidrug resistance

NBF: neutral buffered formalin

NFκB: nuclear factor kappa B

PBS: phosphate-buffered saline

PT: prothrombin time

PXR: pregnane X receptor

ROC: receiver operating characteristic

TNF-α: tumor necrosis factor alpha

γGT: gamma-glutamyltransferase

## Declarations

### Acknowledgments

The authors are grateful to all the HCC patients/healthy volunteers who participated in this study. The authors thank Dr Amit Kumar Ram and Dr Devanatha Desikan for their contribution in performing western blotting and statistical analysis, respectively.

## Author contributions

BV: Conceptualization, Supervision, Formal analysis, Validation, Visualization, Funding acquisition, Writing—original draft, Writing—review & editing. TM: Investigation, Formal analysis. BP: Visualization, Writing—review & editing. All authors read and approved the submitted version.

## Conflicts of interest

The authors declare that they have no conflicts of interest.

## Ethical approval

This study was reviewed and approved by the JIPMER Post-Graduate Monitoring Committee (PGRMC) and the Institute Ethics Committee (IEC) for human studies (JIP/IEC/2018/0282).

## Consent to participate

Written informed consent was obtained from all the participants to participate in the study.

## Consent to publication

Not applicable.

## Availability of data and materials

Data will be shared on reasonable request to the corresponding author.

## Funding

This work was supported by the JIPMER intramural research grant [JIP/Res/Intramural/0282/2018-19]. The funders had no role in study design, data collection and analysis, decision to publish, or preparation of the manuscript.

## Copyright

© The Author(s) 2025.

## Publisher's note

Open Exploration maintains a neutral stance on jurisdictional claims in published institutional affiliations and maps. All opinions expressed in this article are the personal views of the author(s) and do not represent the stance of the editorial team or the publisher.

## References

1. Tan EY, Danpanichkul P, Yong JN, Yu Z, Tan DJH, Lim WH, et al. Liver cancer in 2021: Global Burden of Disease study. *J Hepatol*. 2025;82:851–60. [\[DOI\]](#) [\[PubMed\]](#)
2. Vairappan B, Wright G, Ravikumar TS. Incidence, Diagnosis, and Management of Hepatocellular Carcinoma: Current Perspectives and Future Direction. *J Dig Dis Hepatol*. 2023;8:188. [\[DOI\]](#)
3. Rungay H, Arnold M, Ferlay J, Lesi O, Cabaasag CJ, Vignat J, et al. Global burden of primary liver cancer in 2020 and predictions to 2040. *J Hepatol*. 2022;77:1598–606. [\[DOI\]](#) [\[PubMed\]](#) [\[PMC\]](#)
4. McGlynn KA, Petrick JL, El-Serag HB. Epidemiology of Hepatocellular Carcinoma. *Hepatology*. 2021; 73:4–13. [\[DOI\]](#) [\[PubMed\]](#) [\[PMC\]](#)
5. Yang C, Zhang H, Zhang L, Zhu AX, Bernards R, Qin W, et al. Evolving therapeutic landscape of advanced hepatocellular carcinoma. *Nat Rev Gastroenterol Hepatol*. 2023;20:203–22. [\[DOI\]](#) [\[PubMed\]](#)
6. Feng F, Jiang Q, Cao S, Cao Y, Li R, Shen L, et al. Pregnane X receptor mediates sorafenib resistance in advanced hepatocellular carcinoma. *Biochim Biophys Acta Gen Subj*. 2018;1862:1017–30. [\[DOI\]](#) [\[PubMed\]](#)
7. Mohandas S, Vairappan B. Role of pregnane X-receptor in regulating bacterial translocation in chronic liver diseases. *World J Hepatol*. 2017;9:1210–26. [\[DOI\]](#) [\[PubMed\]](#) [\[PMC\]](#)



8. Mohandas S, Vairappan B. Pregnane X receptor activation by its natural ligand Ginkgolide-A improves tight junction proteins expression and attenuates bacterial translocation in cirrhosis. *Chem Biol Interact.* 2020;315:108891. [DOI] [PubMed]
9. Xing Y, Yan J, Niu Y. PXR: a center of transcriptional regulation in cancer. *Acta Pharm Sin B.* 2020;10:197–206. [DOI] [PubMed] [PMC]
10. Ouyang N, Ke S, Eagleton N, Xie Y, Chen G, Laffins B, et al. Pregnane X receptor suppresses proliferation and tumourigenicity of colon cancer cells. *Br J Cancer.* 2010;102:1753–61. [DOI] [PubMed] [PMC]
11. Kotiya D, Jaiswal B, Ghose S, Kaul R, Datta K, Tyagi RK. Role of PXR in Hepatic Cancer: Its Influences on Liver Detoxification Capacity and Cancer Progression. *PLoS One.* 2016;11:e0164087. [DOI] [PubMed] [PMC]
12. Azuma K, Urano T, Ouchi Y, Inoue S. Vitamin K2 suppresses proliferation and motility of hepatocellular carcinoma cells by activating steroid and xenobiotic receptor. *Endocr J.* 2009;56:843–9. [DOI] [PubMed]
13. Kodama S, Negishi M. Pregnane X receptor PXR activates the *GADD45β* gene, eliciting the p38 MAPK signal and cell migration. *J Biol Chem.* 2011;286:3570–8. [DOI] [PubMed] [PMC]
14. DeLong ER, DeLong DM, Clarke-Pearson DL. Comparing the areas under two or more correlated receiver operating characteristic curves: a nonparametric approach. *Biometrics.* 1988;44:837–45. [DOI] [PubMed]
15. Li Z, Kruijt JK, van der Sluis RJ, Van Berkel TJ, Hoekstra M. Nuclear receptor atlas of female mouse liver parenchymal, endothelial, and Kupffer cells. *Physiol Genomics.* 2013;45:268–75. [DOI] [PubMed]
16. Yoshinari K. Role of Nuclear Receptors PXR and CAR in Xenobiotic-Induced Hepatocyte Proliferation and Chemical Carcinogenesis. *Biol Pharm Bull.* 2019;42:1243–52. [DOI] [PubMed]
17. Shizu R, Ishimura M, Nobusawa S, Hosaka T, Sasaki T, Kakizaki S, et al. The influence of the long-term chemical activation of the nuclear receptor pregnane X receptor (PXR) on liver carcinogenesis in mice. *Arch Toxicol.* 2021;95:1089–102. [DOI] [PubMed]
18. Bhagyaraj E, Ahuja N, Kumar S, Tiwari D, Gupta S, Nanduri R, et al. TGF-β induced chemoresistance in liver cancer is modulated by xenobiotic nuclear receptor PXR. *Cell Cycle.* 2019;18:3589–602. [DOI] [PubMed] [PMC]
19. He J, Gerstenlauer M, Chan LK, Leithäuser F, Yeh MM, Wirth T, et al. Block of NF-κB signaling accelerates MYC-driven hepatocellular carcinogenesis and modifies the tumor phenotype towards combined hepatocellular cholangiocarcinoma. *Cancer Lett.* 2019;458:113–22. [DOI] [PubMed]
20. Taniguchi K, Karin M. NF-κB, inflammation, immunity and cancer: coming of age. *Nat Rev Immunol.* 2018;18:309–24. [DOI] [PubMed]
21. Hoesel B, Schmid JA. The complexity of NF-κB signaling in inflammation and cancer. *Mol Cancer.* 2013;12:86. [DOI] [PubMed] [PMC]
22. Wahli W. A gut feeling of the PXR, PPAR and NF-κB connection. *J Intern Med.* 2008;263:613–9. [DOI] [PubMed]
23. Teng S, Piquette-Miller M. The involvement of the pregnane X receptor in hepatic gene regulation during inflammation in mice. *J Pharmacol Exp Ther.* 2005;312:841–8. [DOI] [PubMed]
24. Feng H, Li B, Li Z, Wei Q, Ren L. PIVKA-II serves as a potential biomarker that complements AFP for the diagnosis of hepatocellular carcinoma. *BMC Cancer.* 2021;21:401. [DOI] [PubMed] [PMC]
25. Jyothi V, Pottakkat B, V B, Verma SK. Serum Levels of Netrin-4 and Its Association With Hepatocellular Carcinoma: Results From a Case-Control Study. *Cureus.* 2023;15:e43844. [DOI] [PubMed] [PMC]
26. Choi S, Neequaye P, French SW, Gonzalez FJ, Gyamfi MA. Pregnane X receptor promotes ethanol-induced hepatosteatosis in mice. *J Biol Chem.* 2018;293:1–17. [DOI] [PubMed] [PMC]